J|A|C|S ARTICLES

Published on Web 02/27/2009

Solvothermal Synthesis and Photoreactivity of Anatase TiO_2 Nanosheets with Dominant {001} Facets

Hua Gui Yang,[†,‡] Gang Liu,[†,§] Shi Zhang Qiao,[*,†] Cheng Hua Sun,[†,||] Yong Gang Jin,[†] Sean Campbell Smith,[†,||] Jin Zou,[⊥] Hui Ming Cheng,[§] and Gao Qing (Max) Lu[*,†]

The University of Queensland, ARC Centre of Excellence for Functional Nanomaterials, Centre for Computational Molecular Science and Centre for Microscopy and Microanalysis, School of Engineering and Australian Institute of Bioengineering and Nanotechnology, QLD 4072, Australia, Key Laboratory for Ultrafine Materials of Ministry of Education, School of Materials Science and Engineering, East China University of Science & Technology, Shanghai 200237, China, and Shenyang National Laboratory for Materials Science, Institute of Metal Research, Chinese Academy of Sciences, 72 Wenhua Road, Shenyang 110016, China

Received November 10, 2008; E-mail: s.qiao@uq.edu.au; maxlu@uq.edu.au

Abstract: Owing to wide-ranging industrial applications and fundamental importance, tailored synthesis of well-faceted single crystals of anatase TiO_2 with high percentage of reactive facets has attracted much research interest. In this work, high-quality anatase TiO_2 single-crystal nanosheets mainly dominated by {001} facets have been prepared by using a water−2-propanol solvothermal synthetic route. The synergistic functions of 2-propanol and HF on the growth of anatase TiO_2 single-crystal nanosheets were studied by first-principle theoretical calculations, revealing that the addition of 2-propanol can strengthen the stabilization effect associated with fluorine adsorption over (001) surface and thus stimulate its preferred growth. By measuring the $^{\bullet}OH$ species with terephthalic acid scavenger, the as-prepared anatase TiO_2 single-crystal nanosheets having 64% {001} facets show superior photoreactivity (more than 5 times), compared to P25 as a benchmarking material.

Introduction

Metallic and semiconducting nanocrystals with tailored shapes have attracted intense research interest in the past decade due to their many intrinsic shape-dependent properties.[1−4] Anatase titanium dioxide (TiO_2) is one of the most important semiconductors, playing a central role in many applications such as photovoltaic cells, photo/electrochromics, photocatalysis, photonic crystals, smart surface coatings, and sensors.[5,6] Theoretical studies indicate that the (001) surface of anatase TiO_2 is much more reactive than the thermodynamically more stable (101) surface and that the (001) surfaces may in fact be the dominant source of active sites for various applications (e.g., photocatalytic production of H_2).[7a,d] Unfortunately, most synthetic anatase crystals, as well as those naturally occurring, are dominated by the less-reactive (101) surface.[7] Furthermore, it appears that there has been no direct experimental evidence showing the reactivity of (001) surfaces, largely due to the difficulty of growing well-defined anatase single crystals rich in {001} facets.[7b]

Very recently, we prepared anatase single crystals with 47% of the highly reactive {001} facets by using hydrofluoric acid (HF) as a capping agent under hydrothermal conditions.[8] However, in order to confirm the reactivity of {001} facets experimentally, TiO_2 single crystals with dominant {001} facets are highly desirable in order to reduce the influence of contributions of {101} facets. To address this fundamental issue, herein we report a new solvothermal method using 2-propanol as a synergistic capping agent and reaction medium together with HF to synthesize high-quality anatase TiO_2 single-crystal nanosheets (SCNSs) with 64% of the {001} facets. Promising photoreactivity of the anatase SCNSs is demonstrated by measuring the rate of $^{\bullet}OH$ formation under UV−vis light

[†] The University of Queensland, ARC Centre of Excellence for Functional Nanomaterials.
[‡] East China University of Science & Technology.
[§] Institute of Metal Research, Chinese Academy of Sciences.
[||] The University of Queensland, Centre for Computational Molecular Science.
[⊥] The University of Queensland, Centre for Microscopy and Microanalysis.

(1) (a) Tian, N.; Zhou, Z. Y.; Sun, S. G.; Ding, Y.; Wang, Z. L. *Science* **2007**, *316*, 732. (b) Yin, Y.; Alivisatos, A. P. *Nature* **2005**, *437*, 664.
(2) Wang, C.; Daimon, H.; Onodera, T.; Koda, T.; Sun, S. *Angew.Chem., Int. Ed.* **2008**, *47*, 3588.
(3) Tao, A. R.; Habas, S.; Yang, P. D. *Small* **2008**, *4*, 310.
(4) Jun, Y.; Choi, J.; Cheon, J. *Angew. Chem., Int. Ed.* **2006**, *45*, 3414.
(5) Fujishima, A.; Honda, K. *Nature* **1972**, *238*, 37.
(6) (a) O'Regan, B.; Grätzel, M. *Nature* **1991**, *353*, 737. (b) Grätzel, M. *Nature* **2001**, *414*, 338. (c) Barbé, C. J.; Arendse, F.; Comte, P.; Jirousek, M.; Lenzmann, F.; Shklover, V.; Grätzel, M. *J. Am. Ceram. Soc.* **1997**, *80*, 3157. (d) Snaith, H. J.; Schmidt-Mende, L. *Adv. Mater.* **2007**, *19*, 3187. (e) Chen, X.; Mao, S. *Chem. Rev.* **2007**, *107*, 2891.
(7) (a) Gong, X. Q.; Selloni, A. *J. Phys. Chem. B* **2005**, *109*, 19560. (b) Diebold, U. *Surf. Sci. Rep.* **2003**, *48*, 53. (c) Barnard, A. S.; Curtiss, L. A. *Nano Lett.* **2005**, *5*, 1261. (d) Vittadini, A.; Selloni, A.; Rotzinger, F. P.; Grätzel, M. *Phys. Rev. Lett.* **1998**, *81*, 2954. (e) Arrouvel, C.; Digne, M.; Breysse, M.; Toulhoat, H.; Raybaud, P. *J. Catal.* **2004**, *222*, 152. (f) Yang, H. G.; Zeng, H. C. *J. Phys. Chem. B* **2004**, *108*, 3492. (g) Yang, H. G.; Zeng, H. C. *J. Am. Chem. Soc.* **2005**, *127*, 270.
(8) Yang, H. G.; Sun, C. H.; Qiao, S. Z.; Zou, J.; Liu, G.; Smith, S. C.; Cheng, H. M.; Lu, G. Q. *Nature* **2008**, *453*, 638.

 10.1021/ja808790p CCC: $40.75

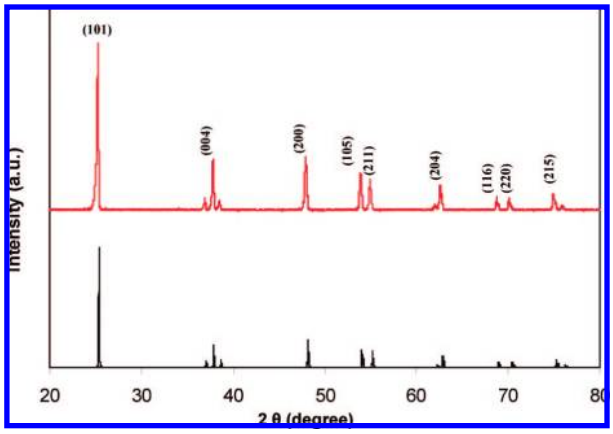

Figure 1. Representative XRD pattern of the as-synthesized anatase TiO_2 SCNSs (top), which is in good agreement with the calculated diffraction pattern of bulk anatase (bottom).

Table 1. Calculated Adsorption Energy (E_{ads}) of the Fluorine Atom over (001) and (101)

surface condition	minimal basis, eV	DNP, eV	DNP + COSMO, eV
clean (001)	3.1	3.1	4.4
Pr-(001)	4.9	4.8	5.2
clean (101)	2.4	2.1	2.8
Pr-(101)	2.3	2.1	2.7

irradiation. We also propose and discuss a plausible reaction mechanism supported by first-principle calculations.

Experimental Methods and Theoretical Calculations

Materials Preparation. Hydrochloric acid (HCl, 1.5 M) was used to adjust the pH of deionized water (1.0 L) to 2.0. Titanium tetrafluoride (TiF_4, Aldrich Chemical) was then dissolved in this solution under vigorous stirring to give a concentration of 0.04 M, during which pH was changed to 1.8.[7f,g,8] Deionized water was used to adjust the concentration. The TiF_4 solution is clear and stable under room temperature. For a typical experiment, 14.5 mL of the above TiF_4 aqueous solution (2.76 mM), 13.38 mL of 2-propanol (PrOH, HPLC grade), and 0.5 mL of hydrofluoric acid (HF, 10% w/w) were added into a Teflon-lined stainless steel autoclave. The autoclave was kept at 180 °C for 5.5−44 h in an electric oven. After reaction, the anatase TiO_2 single-crystal nanosheets were harvested by centrifugation, washed with deionized water 3 times, and then dried in vacuum overnight. The average yield of anatase TiO_2 is 34.8%. The surface fluorine of anatase TiO_2 SCNSs was removed to obtain a clean fluorine-free surface through a heat treatment process at 600 °C for 90 min.

Photoreactivity Measurement. Various photocatalysts including anatase TiO_2 SCNSs and P25 (10 mg) were suspended in 40 mL of aqueous solution containing 0.01 M NaOH and 3.0 mM terephthalic acid. Before exposure to UV−vis light irradiation, the suspension was stirred in the dark for 30 min. Then, 5.0 mL of solution was taken out every 30 min, and the TiO_2 was separated from the solution with a centrifugation method. The remaining clear liquid was used for fluorescence spectrum measurements. During the photoreactions, no oxygen was bubbled into suspension. The employed excitation light in recording fluorescence spectra is 320 nm. The light source employed in photoreactions is a 300 W Xe lamp (PLS-SXE-300UV) equipped with two glass filters, whose emission gives a wavelength of 220−770 nm.

Materials Characterization. The shape and crystal structure of the resulting anatase TiO_2 SCNSs were investigated by X-ray spectroscopy (XRD, Bruker D8 Advanced Diffractometer, Cu Kα radiation, 40 kV), scanning electron microscopy (SEM, JEOL JSM6400F), and transmission electron microscopy and selected area

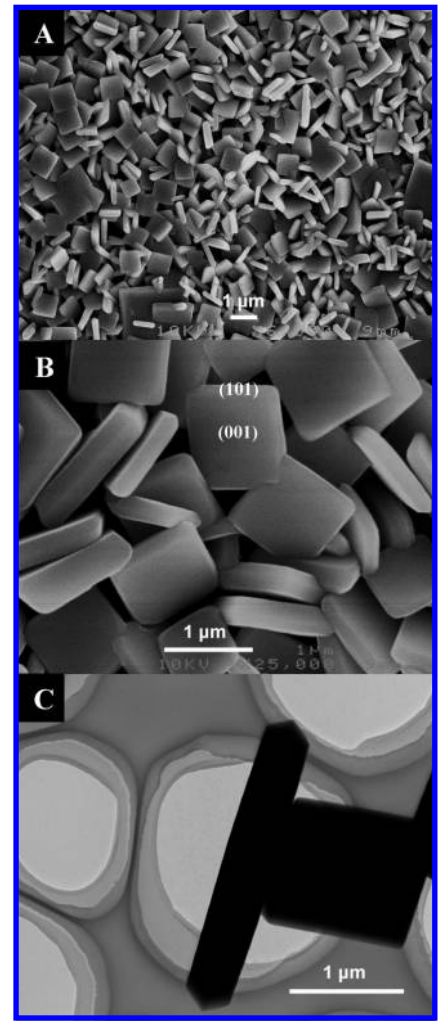

Figure 2. Typical SEM/TEM images (A−C) of the anatase TiO_2 SCNS synthesized with a reaction time of 11 h.

electron diffraction (TEM/SAED, Philips Tecnai T30F FEG Cryo AEM). Chemical compositions of anatase TiO_2 SCNSs were analyzed with X-ray photoelectron spectroscopy (XPS, Kratos Axis ULTRA incorporating a 165 mm hemispherical electron energy analyzer). All binding energies were referenced to the C1s peak (285.0 eV) arising from surface hydrocarbons (or possible adventitious hydrocarbon). Prior peak deconvolution, X-ray satellites, and inelastic background (Shirley-type) were subtracted for all spectra. The chemical bonding status of anatase TiO_2 SCNSs was studied with Fourier transform infrared spectroscopy (FTIR, Nicolet IR 6700) using the potassium bromide (KBr) pellet technique. Nitrogen sorption isotherms were obtained with a Quadrasorb analyzer (Quantachrome) at 77 K, and all the samples were degassed at 120 °C for 12 h under vacuum before any measurements were taken. Samples were centrifuged and washed with deionized water twice and then redispersed in water and dropped on a conductive SEM sample holder or a carbon-coated copper grid with irregular holes for TEM analysis. Samples for XRD, XPS, and FTIR analysis were prepared by drying the sedimented particles overnight at 100 °C.

Theoretical Calculations. Spin-polarized DFT calculations were carried out to investigate the coadsorption profile of fluorine and 2-propanol, based on 4 × 4 slab models with the vacuum thickness being larger than 15 Å. All geometry optimizations and single-point energies were carried out using the local orbital functional method implemented with the Dmol3 package.[9] Exchange and

(9) Delley, B. *J. Chem. Phys.* **2000**, *114*, 7756.

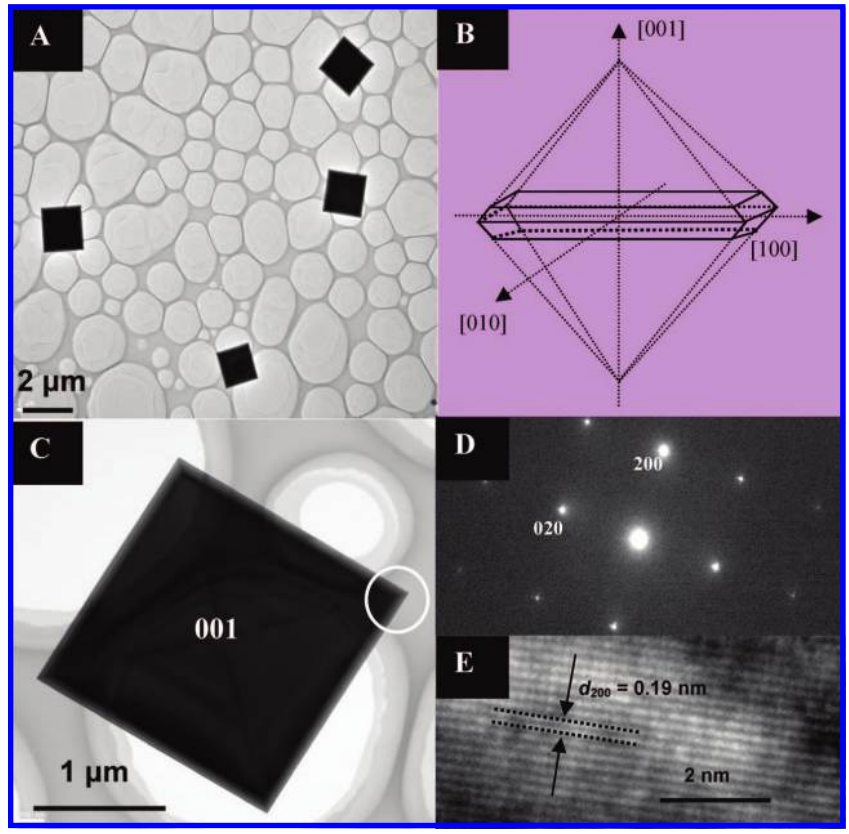

Figure 3. (A) TEM images of the anatase TiO_2 SCNSs synthesized with a reaction time of 22 h. (B) Schematic illustration of the crystal orientation. (D and E) SAED pattern and a high-resolution TEM image of the anatase TiO_2 SCNS shown in the inset of C.

correlation were treated in the generalized gradient approximation (GGA) of Perdew−Burke−Ernzerhof (RPBE).[10] Due to the large size of the slab model, the *k* point is only set as 1 × 1 × 1. All structures were first optimized using a minimal basis set (one atomic orbital for each orbital that is occupied in the free atom) for the preoptimization purpose, then followed by a full optimization using double-numeric quality basis with polarization functions (DNP), approximately two atomic orbitals for each one occupied in the free atom, and all functions were expressed with angular momentum one higher than that of highest occupied orbital in free atom. According to our detailed tests, the difference between the results obtained from minimal basis and DNP was not more than 0.1 eV in terms of adsorption energy, as listed in Table 1. On the basis of the optimized structures, the system was augmented with an implicit water environment; the solvent effect of the water medium was described by the conductor-like screening model (COSMO).[11] COSMO is a continuum solvent model where the solute molecule forms a cavity within the dielectric continuum of permittivity that represents the solvent. The charge distribution of the solute polarizes the dielectric medium. The response of the dielectric medium is described by the generation of screening (or polarization) charges on the cavity surface.

Results and Discussion

In this work, the reaction medium was prepared by mixing aqueous TiF_4 and 2-propanol (PrOH), after which hydrofluoric acid (HF, 10% w/w) was added as capping agent. The crystallographic structure of the as-synthesized crystals has been confirmed by X-ray diffraction (XRD, Cu Kα radiation), and the diffraction pattern in Figure 1 clearly indicates that the sample is a pure anatase phase (tetragonal, $I4_1/amd$, JCPDS 21-1272). Figure 2A−C shows the representative scanning electron microscope (SEM) and transmission electron microscope (TEM) images of the highly truncated bipyramidal anatase TiO_2 SCNSs synthesized for 11 h. From the symmetries of the well-faceted crystal structure of the SCNSs, the two flat square surfaces are identified as {001} facets while the other eight isosceles trapezoidal surfaces are {101} facets (Figure 2B and 2C), which can be also revealed from the interfacial angle with a typical value of 68.3 ± 0.3° (shown in SI-1, Supporting Information).[7b] The average size of the anatase TiO_2 SCNSs is 1.09 μm with a thickness of 260 nm, and the percentage of {001} facets is 64% on average.

TEM images and selected area electron diffraction (SAED) in Figure 3A, 3C, and 3D further confirm the single-crystalline characteristics, and the SAED pattern can be indexed as [001] zone. In addition, the high-resolution TEM image recorded from the white circled area in Figure 3C clearly shows the continuous (200) atomic planes with a lattice spacing of 1.9 Å (Figure 3E), corresponding to the {200} planes of anatase TiO_2 single crystals.[12] A schematic illustration of the crystal orientation of the anatase TiO_2 SCNSs is shown in Figure 3B.

The synergistic functions of chemisorbed F to lower the surface energy[8] and PrOH to act as protective capping agent lead to the formation of anatase TiO_2 SCNSs, which is a thermodynamically favored morphology under these conditions.

(10) Perdew, J. P.; Burke, K.; Ernzerhof, M. *Phys. Rev. Lett.* **1996**, *77*, 3865.

(11) (a) Klamt, A.; Schüürmann, G. *J. Chem. Soc., Perkin Trans.* **1993**, *2*, 799. (b) Klamt, A.; Jonas, V.; Burger, T.; Lohrenz, J. *J. Phys. Chem.* **1998**, *102*, 5074.

(12) (a) Jun, Y. W.; Casula, M. F.; Sim, J.-H.; Kim, S. Y.; Cheon, J.; Alivisatos, A. P. *J. Am. Chem. Soc.* **2003**, *125*, 15981. (b) Penn, R. L.; Banfield, J. F. *Geochim. Cosmochim. Acta* **1999**, *63*, 1549.

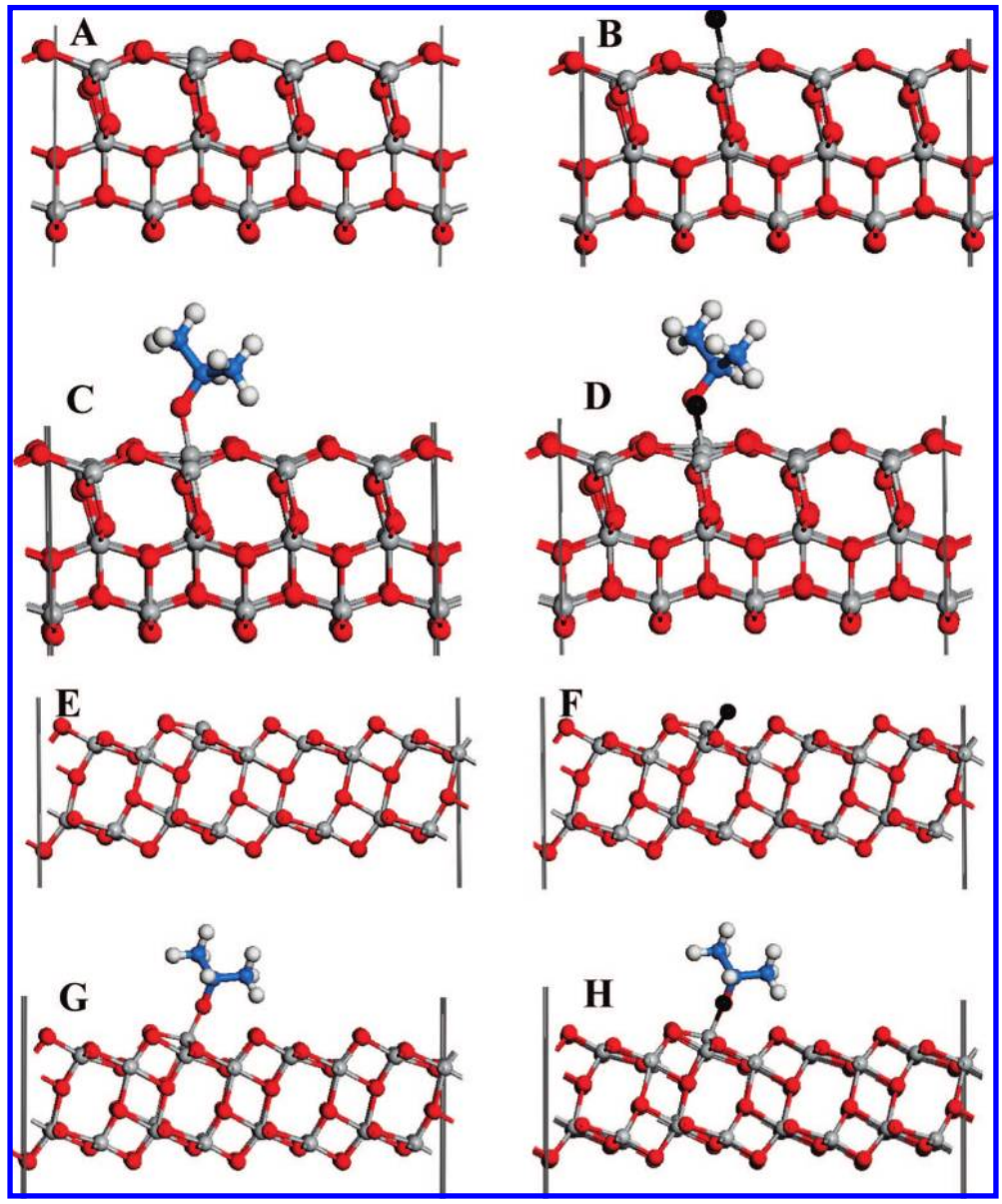

Figure 4. Slab models employed in DFT calculations, with Ti, O, F, and H indicated as gray, red, black, and blue spheres. (A) Clean (001); (B) (001)-F, adsorption of F over (001); (C) (001)-Pr, PrOH modified (001); (D) (001)-F and Pr, adsorption of F over PrOH-modified (001); (E) clean (101); (F) (101)-F, adsorption of F over (101); (G) (101)-Pr, PrOH-modified (101); (H) (101)-F and Pr, adsorption of F over PrOH-modified (101).

The PrOH plays multiple roles in this synthetic system for the formation of anatase TiO_2 SCNSs. It acts not only as reaction medium but also as protecting agent[13] to control the isotropic growth of anatase TiO_2 single crystals because under acidic conditions PrOH tends to heterolytically dissociate to form an alkoxy group ($(CH_3)_2CHO^-$) bound to coordinatively unsaturated Ti^{4+} cations on the (001) and (101) surfaces. The higher density of 5-fold Ti on (001) surfaces may lead to more obvious selective adhesion of PrOH, which retards the growth of anatase TiO_2 single crystals along [001] direction.[12a]

To investigate the synergistic effect resulted by the coadsorption of F and PrOH, density functional theory (DFT) calculations were employed. The effect associated with PrOH on the adsorption of F can be described by the difference of adsorption energy of fluorine atoms over clean and PrOH-modified surfaces. Therefore, for both (001) and (101), two surface conditions are considered, including clean surfaces and PrOH-modified surfaces, as shown in Figure 4A−H. The calculated total energies for all these structures are listed in the Supporting Information (see Table S1), based on which the adsorption energies of fluorine, E_{ads}, were calculated and are listed in Table 1. From the calculated data, it is clearly seen that, in the vacuum, the results obtained from minimal basis and DNP basis are close to each other, suggesting that the employed computational methods exhibit good reliability. With incorporation of the solvent effect, the values of E_{ads} were further corrected with an increment of 0.4−1.3 eV, indicating that the water medium plays an important role on the adsorption of fluorine. Therefore, the data for E_{ads} calculated with the DNP basis and the COSMO solvent model (i.e., the last column of Table 1) were employed in the following analysis.

In the case of clean surfaces, the adsorption energy of F over (001) and (101) is 4.4 and 2.8 eV, respectively (Table 1). This indicates that fluorine prefers to adsorb on the (001) surface,

(13) Yang, H. G.; Zeng, H. C. *Angew. Chem., Int. Ed.* **2004**, *43*, 52069.

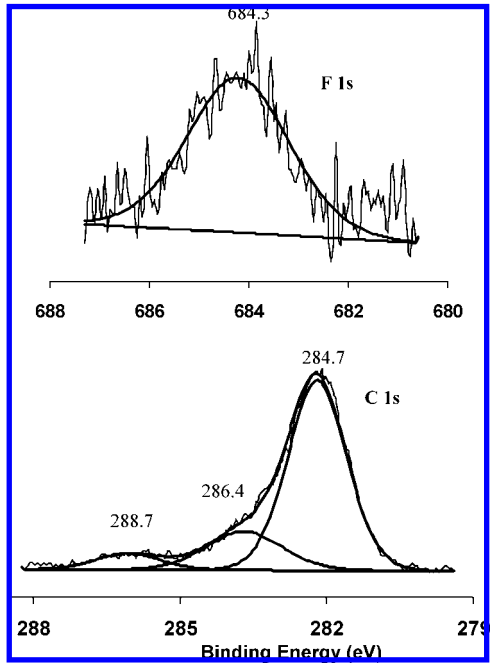

Figure 5. XPS spectra of the representative samples, indicating the existence and bonding status of F and C on the surface of anatase TiO_2 SCNSs.

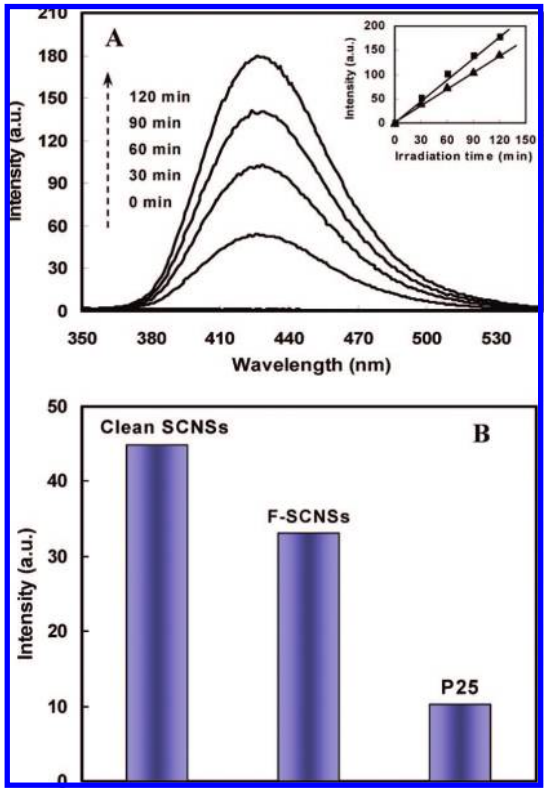

Figure 6. Fluorescence spectra (A) of the UV−vis light (220−770 nm) irradiated TiO_2 SCNSs with fluorine-free surfaces (denoted as clean SCNSs) in 3 mM terephthalic acid at different irradiation times. (B) Normalized fluorescence intensity per unit surface area with different photocatalysts: clean SCNSs, TiO_2 SCNSs capped by F atoms (denoted as F-SCNSs), and Degussa P25 TiO_2.[1a,8] Inset in A is the time dependences of fluorescence intensity at 426 nm, where squares are clean SCNSs and triangles are F-SCNSs, respectively.

which is related to the higher reactivity of the (001) as described in our earlier work.[8] With the modification of PrOH, adsorption energy increases by 0.8 eV for F adsorption over (001) but decreases by 0.1 eV over (101). This difference strongly supports the idea that the coadsorption of PrOH can effectively strengthen the adsorption of fluorine over (001), whereas it slightly weakens the interaction between fluorine and the (101) surface. As indicated above, the essential strategy to achieve predominantly (001) surface area is to reduce its surface energy and kinetically retard its growth relative to the (101), which can be realized by the coverage of fluorine because the bonding of F−Ti can substantially stabilize unsaturated titanium. Therefore, the addition of PrOH can strengthen the stabilization effect associated with fluorine adsorption and thus stimulate the growth of the (001) surface.

The existence and bonding states of F and aliphatic C are shown by the XPS analysis (Figure 5A and 5B). The XPS spectrum of F 1s core electrons shows that the measured bonding energy (BE) is 684.5 eV, which is a typical value for the fluorinated TiO_2 system such as ≡Ti−F species on the TiO_2 crystal surface.[8,14] Similarly, the C 1s spectrum shows a component at a BE of 286.4 eV, which may result from surface oxidation of the aliphatic chains and adsorbed isopropoxide species.[15] The C 1s peak at 284.7 eV can be assigned as aliphatic hydrocarbon, and the smaller peak at BE of 288.7 eV is due to the presence of carboxylate impurities.[16a] To further examine the state of the 2-propanol, the as-synthesized and calcined samples were analyzed with FTIR. The characteristic adsorption band of $-CH_3$ due to anchored surface organics such as 2-propoxide can be observed in the spectrum of the as-synthesized sample (shown in Figure SI-2, Supporting Information), while this band is not present in the spectrum of the calcined sample.[16b] This further confirms the organic cappings of 2-propanol on the anatase TiO_2 SCNSs.

The efficiency for heterogeneous photocatalytic reaction of anatase TiO_2 SCNSs synthesized with a reaction time of 22 h was monitored by measuring the formation of active hydroxyl radicals (•OH) upon irradiation, which are considered as the most important oxidative species in photocatalysis reactions.[17] Terephthalic acid (TA) was used as a fluorescence probe because it can react with •OH in basic solution to generate 2-hydroxy terephthalic acid (TAOH), which emits unique fluorescence signal with the spectrum peak around 426 nm.[14] As shown in Figure 6A, significant fluorescence spectra associated with TAOH were generated upon irradiation within 220−770 nm. The linear relationship between fluorescence intensity and irradiation time (inset of Figure 6A) confirms the stability of anatase TiO_2 SCNSs. The capability of forming •OH per unit surface area of anatase TiO_2 SCNSs or P25, as for the basis for the comparison, is examined in this work. On the basis of the Brunauer−Emmett−Teller (BET) surface area of anatase TiO_2 SCNSs and P25 (1.6 and 47.0 m^2/g, respectively, Supporting Information, Figure SI-3), the normalized concentration of •OH generated from SCNSs with clean surfaces is more than 5 times higher than that of Degussa P25 TiO_2, as seen in Figure 6B. The results clearly demonstrate substantially enhanced photoreactivity of the anatase TiO_2 SCNSs with a large percentage of {001} facets, which can be attributed to the high density of

(14) Yu, J. C.; Yu, J.; Ho, W.; Jiang, Z.; Zhang, L. *Chem. Mater.* **2002**, *14*, 3808.
(15) Farfan-Arribas, E.; Madix, R. J. *J. Phys. Chem. B* **2002**, *106*, 10680.
(16) (a) Yao, K. X.; Sinclair, R.; Zeng, H. C. *J. Phys. Chem. C* **2007**, *111*, 2032. (b) Xu, W.; Raftery, D.; Francisco, J. S. *J. Phys. Chem. B* **2003**, *107*, 4537.
(17) Hsutomu, H.; Nosaka, Y. *Langmuir* **2002**, *18*, 3247.

unsaturated 5-fold Ti as well as their unique electronic structure.[7a,b,d]

Conclusions

We demonstrated a new solvothermal synthetic route for morphology-controlled preparation of high-quality anatase TiO_2 single crystals using 2-propanol as a synergistic capping agent and reaction medium together with HF. The roles of 2-propanol and HF in facilitating the growth of anatase SCNSs were explored by first-principle theoretical calculations, revealing that the presence of 2-propanol can enhance the stabilization effect associated with fluorine adsorption over the (001) surface. Thus, we construe that a synergistic functionality of chemisorbed F to lower the (001) surface energy and 2-propanol to enhance this stabilization and act as protective capping agent leads to the formation of anatase TiO_2 SCNSs, which is a thermodynamically favored morphology under these conditions. Statistically, the synthesized SCNSs have 64% {001} facets and display superior photoreactivity (more than 5 times) compared to P25 as a benchmarking material. The synthetic strategy used in this work may potentially be extendable to other metal oxides such as ZnO, SnO_2, Co_3O_4, and CuO to generate well-defined crystallographic facets of choice.

Acknowledgment. This work was financially supported by the Australian Research Council (ARC) through Discovery Project program, UQ Middle Career Research Fellowship for SZQ, the ARC Centre of Excellence for Functional Nanomaterials, Scientific Research Foundation from East China University of Science & Technology, and Ministry of Science and Technology of China (No. 2009CB220001). We acknowledge generous grants of high-performance computer time from both the Computational Molecular Science cluster computing facility at The University of Queensland and the Australian Partnership for Advanced Computing National Facility.

Supporting Information Available: Crystallographic angle measurement, FTIR spectra of the as-synthesized and calcined samples, nitrogen adsorption isotherm of anatase TiO_2 SCNSs, and calculated single-point energies in Hatrees. This material is available free of charge via the Internet at http://pubs.acs.org.

JA808790P